ELSEVIER

Journal of Nuclear Materials 290–293 (2001) 459–463

journal of nuclear materials

www.elsevier.nl/locate/jnucmat

Surface effects on plasma-driven tritium permeation through metals

O.V. Ogorodnikova *

Nuclear Fusion Institute RRC 'Kurchatov Institute', Pl. Kurchatova 1, Moscow 123 182, Russia

Abstract

The model for the plasma-driven tritium permeation proposed by Doyle and Brice [J. Vac. Sci. Technol. A 5 (4) (1987) 2311] and by Waelbroeck et al. [Forschungazentrum, Julich, Germany, Jul-1996, 1984] has been developed. An improved analytical expression for the plasma-driven tritium permeation in the steady state is presented. Using the presented analytical expression, the influence of surface conditions on the front and the back sides of a metal has been considered for the plasma-driven permeation of tritium through both endothermic and exothermic metals. The presented pictures allow us to define the steady-state tritium permeation in a wide range of the surface conditions: as for an absolutely clean surface and a bare (presence of small amounts of impurities) surface as for contaminated with different impurities surface. This result can be useful for choosing the plasma-facing material for the future steady-state fusion device. © 2001 Elsevier Science B.V. All rights reserved.

Keywords: Tritium; Permeation; Sticking coefficient

1. Background

Analytical descriptions of the steady-state hydrogen permeation through metals of interest in fusion reactor applications have been done in [1–5]. The model includes the hydrogen penetration from the plasma into the metal to the depth R_p which calls the implantation range, hydrogen diffusion and thermodesorption by recombination of two atoms from the front and the back surfaces:

$$2K_r^0 u_0^2 + 2K_r^L u_L^2 = I_0, \tag{1}$$

$$2K_r^0 u_0^2 = D(u_p - u_0)/R_p, \tag{2}$$

$$2K_r^L u_L^2 = D(u_p - u_L)/(L - R_p), \tag{3}$$

where u_p and u_0 and u_L are the maximum hydrogen concentrations on the depth R_p and hydrogen concentrations on the front and the back sides (Fig. 1), respectively, I_0 is the incoming (non-reflected) hydrogen flux and $D = D_0 \exp(-E_m/kT)$ is the hydrogen diffusion coefficient (E_m is the activation energy for diffusion). The re-emission flux is $J_0 = 2K_r^0 u_0^2$ (at. m^{-2} s^{-1}) and the permeation flux is $J_L = 2K_r^L u_L^2$ (at. m^{-2} s^{-1}) (Fig. 1). The recombination coefficient is defined by a sticking coefficient $s = s_0^* \exp(-2E_c/kT)$ (E_c is the activation energy for chemisorption) which is a function of the surface conditions

$$K_r = s\mu/K_s^2, \tag{4}$$

where $\mu = 1/\sqrt{2\pi mkT}$ (m is the mass of hydrogen molecule and k is Boltzmann's coefficient) and $K_s = K_{s0} \exp(-Q_s/kT)$ is solubility (Q_s is the heat of solution). The sticking coefficient is a function of the structure of the surface, crystallographic orientation of the surface and presence of impurities (like O, S or C) on the surface. Consequently, the sticking coefficient is responsible for the influence of surface conditions on the recombination coefficient and, from this, on the hydrogen thermodesorption rate.

---

[*] Present address: Max-Planck-Institut für Plasmaphysik, Boltzmannstraße 2, D-85748 Garching, Germany.

E-mail addresses: olga.ogorodnikova@ipp.mpg.de, olga@plasma.mephi.ru (O.V. Ogorodnikova).

PII: S0022-3115(00)00642-5

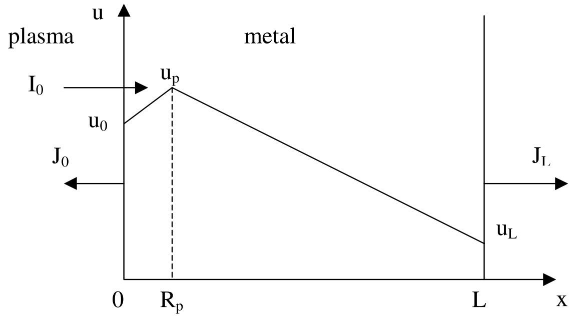

Fig. 1. Schematic of the tritium steady-state concentration in a metal under the plasma/metal interaction. The various parameters listed are defined in the text.

In [6] it was shown that Eqs. (1)–(3) can be reduced to

$$J_L/I_0 = t\sqrt{1 - J_L/I_0} - t\sqrt{K_r^0/K_r^L}\sqrt{J_L/I_0} + \alpha, \qquad (5)$$

where $\alpha = R_p/L$ and $t = J_L^{\mathrm{dif}}/I_0$. Here, $J_L^{\mathrm{dif}} = (D/L)\sqrt{I_0/2K_r^0}$ is the plasma-driven hydrogen permeation in the regime where the diffusion is the slowest step for hydrogen permeation through a metal [6]. Taking into account Eq. (4), the approximation of Eq. (5) is

$$J_L/I_0 = (t^2/4\gamma)\left(\sqrt{1 + (4\gamma/t) + (4\gamma\alpha/t^2)} - 1\right)^2. \qquad (6)$$

The permeation flux divided by the incoming (non-reflected) flux from the plasma, $\eta = J_L/I_0$, we will call the permeation probability. In Eq. (6):

- $t = J_L^{\mathrm{dif}}/I_0$ is the permeation probability in the diffusion-limited regime,
- $\gamma = s_L/(s_0 + s_L)$ is the permeation probability in the surface-limited regime, and
- $\alpha = R_p/L$ is the permeation probability in the implantation-limited regime.

The simple approximations of Eqs. (1)–(3) were derived in [1] and [2], respectively:

$$\eta^{\mathrm{D}} = J_L/I_0 = \gamma(\alpha + t)/(\gamma + \alpha + t), \qquad (7)$$

$$\eta^{\mathrm{BD}} = J_L/I_0 = \left(\gamma'' t^2/(2+t)^2\right)\left(\sqrt{1 + 2(2+t)(\alpha+t)/\gamma'' t^2} - 1\right)^2, \qquad (8)$$

where $\gamma'' = s_0/s_L$.

However, the approximation (7) gives the lower permeation than the exact numerical solution of Eqs. (1)–(3) for simultaneously small t and $\alpha > \gamma$. The approximation (8) results in a higher permeation than the numerical solution for simultaneously high t and γ. On the contrary, Eq. (6) coincides with the numerical solution of Eqs. (1)–(3) for all set of parameters and for this reason it is more general.

Knowledge of the surface composition of real tokamak walls is lacking and it is a main reason for uncertainty in this area. In this paper, we investigate the dependence of the tritium steady-state permeation on the surface conditions on the front, s_0, and the back, s_L, sides.

2. Physical data and operating conditions used in the calculations

Depending on the design and operating conditions, the typical thickness of the first wall ranges from 3 to 10 mm, temperature ranges from 500 to 800 K, incident D/T flux ranges from 10^{19} to 10^{21} (at. m^{-2} s^{-1}) and energy of the incident D/T particles ranges from few eV to few keV (average energy 100–200 eV [7]). For the calculations of the steady-state permeation, a tritium flux $I_0 = 1.5 \times 10^{20}$ at. m^{-2} s^{-1} impinging the plasma-facing side of a material and the metal thickness of $L =$ 5 mm were taking from [8] for the first wall (MANET) of helium-cooled pebble bed blanket (HCPB) originally designed for a DEMO reactor. The mean projected range was assumed to be $R_p \approx 5$ nm [8]. The operating conditions and design parameters for the first wall of the DEMO reactor are given in Table 1. For simplicity, we assume that the reflection coefficient equals to 0. This means that all incident tritium flux, I_0, penetrates into the metal. The data of hydrogen isotope diffusivity and solubility are presented in Table 2. The extrapolated value of tritium is defined using the classical diffusion theory $D_i/D_j = \sqrt{m_j/m_i}$, where i and j are two hydrogen isotopes.

3. Calculations and discussion

More or less accurate information is available for the bulk material properties, diffusivity and solubility, but a small information is available about the surface properties. Even qualitative estimates of the tritium retention and permeation are unreliable without knowledge of the real material surface in future fusion reactors. The dynamic sputtering of surface contaminants may be compensated by the redeposition of sputtering atoms on the metal and by chemical reactions with residual gases. The increase of impurities on the plasma-facing side because

Table 1
Assumed operating conditions and design parameters for the first wall for the DEMO reactor [8]

Tritium incident flux impinged the first wall from the plasma	$I_0 \approx 1.5 \times 10^{20}$ at. m^{-2} s^{-1}
Average energy of the incident flux	$E_i \approx 200$ eV
Implantation depth	$R_p \approx 5 \times 10^{-9}$ m
Metal thickness	$L = 5 \times 10^{-3}$ m

Table 2
Data of diffusivity, $D = D_0 \exp(-E_m/kT)$, and solubility, $K_s = K_{s0} \exp(-Q_s/kT)$, of hydrogen isotopes for several fusion reactor materials

Materials	Diffusivity		Solubility	
	D_0 (m^2 s^{-1})	E_m (eV)	K_{s0} (at. m^{-3} $\sqrt{Pa}$) × 10^{23}	Q_s (eV)
H_2/α-Fe [13]	3.87×10^{-8}	0.045	6.14	0.27
D_2/F82H [14]	1.07×10^{-7}	0.144	4.54	0.278
D_2/MANET [14]	1.01×10^{-7}	0.137	3.25	0.276
D_2/99.8%Be [15]	6.7×10^{-9}	0.3	–	–
T_2/Be [16]	–	–	0.23	0.173
H_2/W [17]	4.1×10^{-7}	0.39	17.7	1.03
H_2/Cu [18]	1.1×10^{-6}	0.4	4.1	0.37
H_2/α-V [19]	3.5×10^{-8}	0.05	1.51	−0.34
H_2/α-Ta [19]	4.4×10^{-8}	0.14	1.5	−0.35
H_2/α-Ti [19,20]	1.45×10^{-6}	0.55	5.2	−0.47
D_2/BeO [21]	1.31×10^{-9}	1.335		
BeO [22]			9.4×10^{-6}	−0.8
H_2/TZM [23]	5.5×10^{-5}	0.88	8.5×10^{-3}	−0.12
H_2/Sn(l) [19]	1×10^{-4}	0	6.2×10^{2}	1.28
H_2/Sn(l) [19]	1×10^{-5}	0		
T_2/Pb-17Li(l) [24]	2.33×10^{-8}	0.195	8.433×10^{-3}	0.0135
H_2/Nb [25]	1.1×10^{-7}	0.147	1.53	−0.366
D_2/Ni [26,27]	4.76×10^{-7}	0.4	4.71	0.15

of the surface segregation of impurities or reactions with residual gases of vacuum system decreases the recombination coefficient and enhances tritium permeation by orders of magnitude. If the energy of the incident particles will be below 50 eV, the much sputtering of impurities from the plasma-facing side is not expected. If the energy of the incident particles striking the first wall will be high enough to remove surface impurities, it is expected that the plasma-facing side will be sputter-cleaned during the plasma operation [9–12]. Removal of the impurities from the front side of the metal increases the front sticking coefficient. The creation of surface roughness and damages have additional effects on the increase of the sticking factor. Consequently, the plasma-facing surface will depend upon the whole set of physical and physico-chemical conditions existing in each particular fusion device. The state of the plasma-facing side may be ranged from sputter-cleaned, $s_0 \to 1$, to very dirty, $s_0 \ll 1$. Because there is no information about the real surface in the future steady-state fusion reactor, the influence of various surface conditions on tritium permeation is considered.

Fig. 2 shows the tritium permeation probability as a function of the surface conditions on the plasma-facing side. The back side is assumed to be slightly contaminated. Sticking coefficients for a bare (slightly contaminated) surface for various metals are presented in Table 3.

The removal of impurities on the plasma-facing side, namely the increase of s_0, significantly decreases tritium permeation and drives the permeation through most of endothermic metals to the implantation-limited regime.

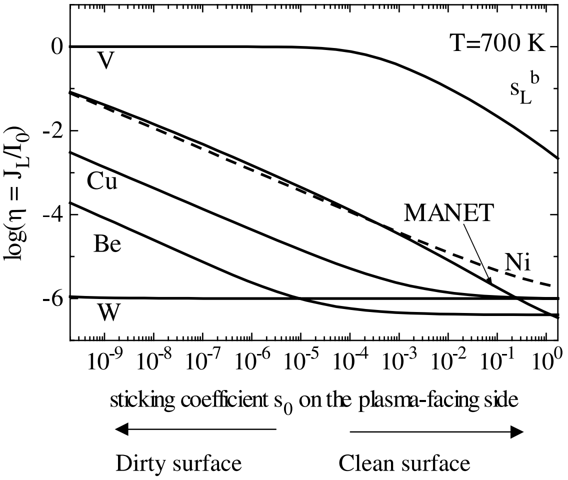

Fig. 2. Tritium permeation probability as a function of the sticking coefficient on the plasma-facing side for a bare (slightly contaminated) back side. Operating conditions and design parameters are given in Table 1. Sticking coefficients for various metals with a bare surface are presented in Table 3.

The steady-state permeation through W is implantation-limited, $\eta = \alpha = R_p/L$, in a wide range of the surface conditions. This means that the surface conditions do not influence the tritium permeation through W.

The increase of impurities on the plasma-facing side, namely the reduction of the front sticking coefficient, s_0, drastically increases hydrogen isotope permeation through most of the endothermic metals (MANET, Ni,

Table 3
Data of the sticking coefficient, $s = s_0 \exp(-2E_c/kT)$, derived from experimental measurements, s^b, for a bare (slightly contaminated) metal surface and calculated by the expression (9), $s^{\text{real\_cl}}$, for a clean metal surface

Metal	Experimental s^b sticking coefficient for a bare surface		Calculated $s^{\text{real\_cl}}$ sticking coefficient for a clean surface ($E_c = 0$)
	(s_0^*)	E_c (eV)	$(s_0^*)^{\text{cl}}$
MANET [14]	$\approx 6.9 \times 10^{-6}$	0.099	$\approx 8 \times 10^{-3}$
Be [7]	$\approx 3 \times 10^{-7}$	0.313	$\approx 3 \times 10^{-5}$
BeO [28]	2.12×10^{-19}	1.09	$\approx 8.6 \times 10^{-16}$
W (1 1 1) [29]	0.25	–	≈0.7
W (1 0 0) [29]	0.18	–	–
W (1 1 0) [29]	0.07	–	–
Mo (1 1 1) [30]	0.7	–	≈0.2
Mo (1 0 0) [30]	0.7	–	–
Mo (1 1 0) [30]	0.35	–	–
TZM	–	–	$\approx 3 \times 10^{-3}$
Cu [6]	≈0.08	0.32	≈0.1
Ti	–	–	0.2
V [31]	1	0.16	4×10^{-4}
Ta	–	–	5×10^{-4}

Cu, Be) but has less influence on the permeation through exothermic metals (V, Nb, Ta, Ti), where the permeation can reach the saturation ($J_L \approx I_0$) already for a slightly contaminated plasma-facing surface.

Physically, the explanation of the increase of the steady-state permeation with the reduction of the sticking coefficient on the front side, is very simple. Impurities on the plasma-facing side act as a barrier against the tritium re-emission. The reduction of s_0 results in the reduction of the re-emission flux: $J_0 = (2s_0\mu/K_s^2)u_0^2$. In the steady state the sum of the re-emission and the permeation fluxes is constant: $I_0 = J_0 + J_L$. If the re-emission flux decreases, the permeation flux increases. On the other hand, the presence of impurities on the back side (reduction of s_L) results in the reduction of the probability of tritium atoms to recombine into molecule to be released from the back surface as a permeation flux. Consequently, the tritium permeation decreases.

Fig. 3 shows the tritium permeation through metals with sputter-cleaned plasma-facing side as a function of the sticking coefficient on the back side. The sticking coefficient for a clean metal surface ($E_c = 0$), can be *roughly* evaluated by the following expression [6]:

$$s^{\text{real\_cl}} = (s_0^*)^{\text{cl}} \approx D_0 K_{s0}^2 \lambda^2/\mu, \qquad (9)$$

where λ is the lattice parameter and $\mu = 1/\sqrt{2\pi m_T kT}$. The sticking coefficients for sputter-cleaned surface for various metals are given in Table 3.

The reduction of impurities (the increase of s_L) on the back side strongly increases the tritium permeation through exothermic metals but only slightly increases the tritium permeation through endothermic metals where the sticking coefficient on the front side has a dominating effect.

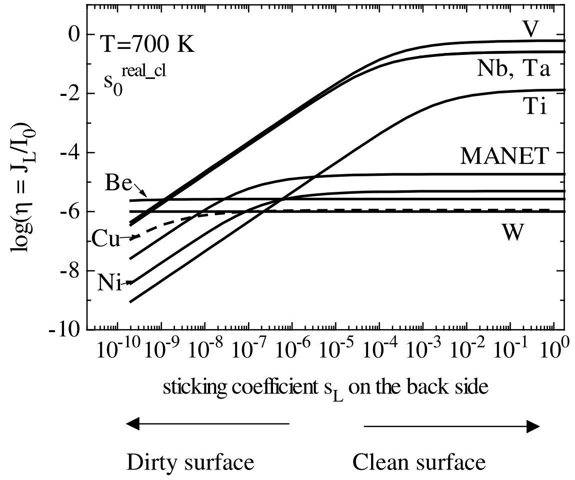

Fig. 3. Tritium permeation probability as a function of the sticking coefficient on the back side for a clean plasma-facing side. Operating conditions and design parameters are given in Table 1. Sticking coefficients for various metals with a clean surface are presented in Table 3.

4. Summary

The assessments of the tritium permeation are required to support safety and environmental studies of future steady-state fusion reactor. An improved approximation of the steady-state plasma-driven permeation of tritium through metals has been presented. Two groups of metal, endothermic and exothermic, have been considered. As the surface conditions are unknown in the future fusion reactors, the dependence of the tritium permeation on different surface conditions has been presented. Both the removal of the surface impurities on the plasma-facing side and the increase of the contamination on the back side reduce the tritium permeation. The non-metal monolayer on the plasma-facing side acts as a barrier against tritium re-emission and, consequently, enhances the tritium permeation and is undesirable.

The tritium permeation through exothermic metals is much higher than through endothermic metals. However, the permeation through exothermic metals may be considerably reduced by contamination (e.g., by oxidation) on the back side. Conversely, the reduction of the sticking coefficient on the back side has less influence on the permeation for endothermic metals where the sticking coefficient on the front side has a dominating influence.

References

[1] B.L. Doyle, J. Nucl. Mater. 111–112 (1982) 635.
[2] D.K. Brice, B.L. Doyle, J. Vac. Sci. Technol. A 5 (4) (1987) 2311.
[3] I. Ali-Khan, K.J. Dietz, F.G. Waelbroeck, P. Wienhold, J. Nucl. Mater. 76–78 (1978) 337.
[4] F. Waelbroeck, P. Wienhold, J. Winter, E. Rota, T. Banno, Forschungazentrum, Jülich, Germany, Jul-1966, 1984.
[5] A.I. Livshits, M.E. Notkin, A.A. Samartsev, J. Nucl. Mater. 170 (1990) 79.
[6] O.V. Ogorodnikova, J. Nucl. Mater. 277 (2000) 130.
[7] G. Federici, D. Holland, J. Brooks, R. Causey, T.J. Dolan, G. Longhurst, IEEE 16th Symposium on Fusion Engineering, vol. 1, 1995, p. 418.
[8] L. Berardinucci, M. Dalle Donne, Fus. Technol. 2 (1997) 1427.
[9] R.A. Anderl, D.F. Holland, D.A. Struttmann, G.R. Longhurst, B.J. Merrill, Tritium permeation in stainless steel-structures exposed to plasma ions, INEL, IEEE (1986) 644.
[10] R.A. Anderl, D.F. Holland, G.R. Longhurst, J. Nucl. Mater. 176&177 (1990) 638 (and references therein).
[11] T. Nagasaki, R. Yamada, M. Saidoh, H. Katsuta, J. Nucl. Mater. 151 (1988) 189.
[12] J. Winter, F. Waelbroeck, P. Wienhold, T. Schelske, J. Nucl. Mater. 111&112 (1982) 243.
[13] K.S. Forcey, I. Iordanova, D.K. Ross, Mater. Sci. Technol. 6 (1990) 357.
[14] E. Serra, A. Perujo, J. Nucl. Mater. 240 (1997) 215.
[15] E. Abramov, M.P. Riehm, D.A. Thompson, W.W. Smeltzer, J. Nucl. Mater. 175 (1990) 90.
[16] V.I. Shapovalov, Ju. Dukel'skii, Russ. Metallkd. 5 (1988) 201.
[17] R. Frauenfelder, J. Vac. Sci. Techol. 6 (1969) 388.
[18] K.L. Wilson, R. Bastasz, R.A. Causey, D.K. Brice, B.L. Doyle, W.R. Wampler, W. Moller, B.M.U. Scherzer, T. Tanabe, Suppl. J. Nucl. Fus. 1 (1991) 31.
[19] E. Fromm, E. Gebhardt (Eds.), Gase und Kohlenstoff in Metallen, Springer, Berlin, 1976.
[20] S. Yamanaka, T. Tanaka, S. Tsuboi, M. Miyake, Fus. Eng. Des. 10 (1989) 303.
[21] G. Longhurst, R.A. Andrel, T.J. Dolan, M.J. Mulock, Fus. Technol. 28 (3) (1995) 1217.
[22] R.G. Macaulay-Newcombe, D.A. Thompson, J. Nucl. Mater. 212–215 (1994) 942.
[23] S. Tominetti, M. Caorlin, J. Camposilvan, A. Perujo, F. Reiter, J. Nucl. Mater. 176&177 (1990) 672.
[24] F. Reiter, J. Camposilvan, G. Gervasini, R. Rota, in: Proceedings of the 14th Symposium on Fusion Technology, Avignon (F), 1986, p. 1185.
[25] M. Yamawaki, T. Namba, K. Yamaguchi, T. Kiyoshi, Nucl. Instrum. Meth. Phys. Res. B 23 (1987) 498.
[26] W. Eichenauer, W. Loser, H. Witte, Z. Metallkd. 56 (1965) 287.
[27] L. Katz, M. Guinan, T.J. Borg, Phys. Rev. B 4 (1971) 330.
[28] S. Cho, A.R. Raffay, M.A. Abdou, J. Nucl. Mater. 212–215 (1994) 961.
[29] P.W. Tamm, L.D. Schmidt, J. Chem. Phys. 55 (N9) (1971) 4253.
[30] R. Chappell, D.O. Hayward, J. Vacuum, Sci. Technol. 9 (1972) 1052.
[31] M. Yamawaki, K. Yamaguchi, S. Tanaka, T. Namba, T. Kiyoshi, Y. Takahashi, J. Nucl. Mater. 162–164 (1989) 1071.